A robust approach to optimal matched filter design in ultrasonic non-destructive evaluation (NDE)

Minghui Li and Gordon Hayward

Citation: AIP Conference Proceedings **1806**, 140002 (2017); doi: 10.1063/1.4974717
View online: http://dx.doi.org/10.1063/1.4974717
View Table of Contents: http://aip.scitation.org/toc/apc/1806/1
Published by the American Institute of Physics

A Robust Approach to Optimal Matched Filter Design in Ultrasonic Non-Destructive Evaluation (NDE)

Minghui Li [1, a)] and Gordon Hayward [2]

[1]*School of Engineering, University of Glasgow, Glasgow G12 8QQ, United Kingdom*
[2]*Alba Ultrasound, Unit 1, Block 3, Todd Campus, West of Scotland Science Park, Glasgow G20 0XA, United Kingdom*

[a)]Corresponding author: minghui.li@ieee.org

Abstract. The matched filter was demonstrated to be a powerful yet efficient technique to enhance defect detection and imaging in ultrasonic non-destructive evaluation (NDE) of coarse grain materials, provided that the filter was properly designed and optimized. In the literature, in order to accurately approximate the defect echoes, the design utilized the real excitation signals, which made it time consuming and less straightforward to implement in practice. In this paper, we present a more robust and flexible approach to optimal matched filter design using the simulated excitation signals, and the control parameters are chosen and optimized based on the real scenario of array transducer, transmitter-receiver system response, and the test sample, as a result, the filter response is optimized and depends on the material characteristics. Experiments on industrial samples are conducted and the results confirm the great benefits of the method.

INTRODUCTION

Reliable and robust defect detection is a challenging yet essential problem in ultrasonic non-destructive evaluation (NDE). The flaw echoes are usually contaminated by high-level, time-invariant, and correlated grain noise originating from the material microstructure. This phenomenon becomes even worse when inspecting coarse grain materials like stainless steels, alloys, carbon-reinforced composites and concrete, which however, forms some of the most important and commonly used industrial materials. A wide variety of techniques have been investigated to enhance flaw detection by exploring either the spatial diversity, e.g. transducer array beamforming [1, 2] and phase coherence imaging [3], or the time-frequency signature and characteristics of the broadband ultrasonic signals, e.g. frequency compounding [4] and matched filtering [5, 6].

The matched filter is known to be optimal in terms of the SNR improvement if the signal waveform and noise statistics are exactly known *a priori*; this is unfortunately not the case in ultrasonic NDE, where either the exact waveform of the echoes returned from the defect or the statistics of the noise, due to electronic circuits, grain noise originating from the material microstructure boundaries or the coupling variation between the transducer and the test sample, is unknown. Earlier studies use simulated flaw signals [7, 8] or the superposition of actual excitation signals [5, 6] to design the filter, but they are inevitably subject to significant errors, especially in NDE of coarse grain materials, where it is quite challenging to simulate a flaw signal to certain extent of similarity [8]. In the literature, the excitation signal measured in the experiments have also been used to design the matched filter, but the procedure is time consuming, or requires extra instrument to exactly record the transmitted signal, and thus not straightforward to implement in practice

In this paper, we propose a flexible and robust method to optimal matched filter design. The excitation waveform is modelled as a broadband signal centered at the transducer frequency with a particular bandwidth which are determined from the ultrasonic array transducer to be used in the experiments; the flaw echo is modelled as the superposition of multiple transmit waveforms with different control parameters like time delay, amplitude gain, and phase shift; and a numerical optimization paradigm is utilized to search the optimal parameters in the above model with an objective to maximize the SNR improvements over a set of training signals captured from the real samples.

43rd Annual Review of Progress in Quantitative Nondestructive Evaluation, Volume 36
AIP Conf. Proc. 1806, 140002-1–140002-10; doi: 10.1063/1.4974717
Published by AIP Publishing. 978-0-7354-1474-7/$30.00

Different from the traditional matched filters used in radar or sonar applications, our filter is designed to match the flaw echoes rather than the excitation signals. As a result, the optimal matched filter depends on the material characteristics and is supposed not identical for different type of materials. The design is validated with experiments on nickel-steel alloy samples, which demonstrates great improvement on the SNR of A-scan waveforms, as well as in the images created by the total focusing method (TFM) with filtered data. The optimal matched filter designed using simulated excitation waveforms illustrate the same performance advantages as those filters designed using the real excitation signals, but requires much less efforts, which makes the proposed method more robust and attractive. Furthermore, the extra computational cost in implementation of the matched filter is low, which makes it ideal for real-time applications.

DATA MODEL

This section describes the ultrasonic array data model, which is used for the optimal matched filter design. The ultrasonic data generated by a transducer array of N elements are usually represented by a complete set of N by N time-domain signals from all combinations of transmit and receive elements, which are referred to as the Full Matrix Capture (FMC) dataset. Each individual time domain trace from a pair of transmit (tx) and receive (rx) elements means the echoes received by the rx element due to the illumination from the tx element into the media.

If there is a single point reflector in a homogeneous and lossless propagation media, the return signal $x(t)$ at the rx element is equal to the signal transmitted from the tx element $s_0(t)$ except for a time delay t and scaling A,

$$x(t) = As_0(t - t_0). \tag{1}$$

The propagation distance from the tx element to the point reflector and back to the rx element can be calculated from the coordinates of the reflector and the transmit and receive elements. And the propagation time, or time delay t_0, is determined by dividing the propagation distance by the longitudinal velocity of sound in the media. The amplitude scaling factor A is employed to address the effects of element directivity and beam spread, as well as the effect of the divergence of the waves from the tx element and from the point reflector. This point reflector signal model is straightforward to follow, and has been used in a variety of literature on radar [9, 10], communications [11, 12], and ultrasonic imaging [13] as a standard data model.

However, in most practical ultrasonic NDE applications, the defects cannot be simply represented by single or well isolated point reflectors; instead most defects are spatially extended and distributed with a spatial shape or profile. A reasonable extension to the above data model for a distributed defect is that the defect consists of a number of point-like reflectors, each with given scaling and characteristics due to the effect of element directivity, beam spread, and spatial position that determines the propagation time. For a spatially extended defect, the return signal $x(t)$ received at the rx element is then given by a sum of J delayed and scaled versions of the transmitted signal $s_0(t)$,

$$x(t) = \sum_{i=1}^{J} A_i s_0(t - t_i) + n(t), \tag{2}$$

where $s_0(t)$ is the excitation signal taking into account of the transmitter output waveform and the frequency response of the transducer, J is the number of point-like reflectors under consideration for this particular extended defect, A_i and t_i are the amplitude factor and the propagation time delay corresponding to a particular point reflector i with certain position and reflection characteristics, and $n(t)$ is the additive noise due to the transceiver internal circuit noise, the environment noise in the media, and the coupling variation, which is assumed to be uncorrelated with the defect signals.

ROBUST AND OPTIMAL MATCHED FILTER DESIGN

As shown in the data model (2), the return echoes originating from a defect is contaminated with noise, which may consists of the electronic noise in the transmitter/receiver channel circuits, the large amount of reflections from the microstructure grain boundaries within the test sample, the coupling variation noise between the transducer and the sample, and etc; and the noise could be significant with regard to the signal of interest originating from the defect, and thus results in a poor SNR. The matched filter is to pass the echoes at the receiver through a filter with a particular response to remove the noise and enhance the SNR. Assume $x(t)$ is a return echo from a distributed defect received by a transducer, and $x(t)$ is processed by a matched filter with a response $h(t)$, the output signal $y(t)$ is then given by

$$y(t) = x(t) * h(t), \tag{3}$$

where * stands for the convolution operation. $x(t)$ is composed of signal components which is determined by the defect profile and characteristics (shape and reflection factor) as well as the additive noise, as illustrated in the data model (2). Based on the theory of matched filtering, if the filter response $h(t)$ is exactly matched to the echo signal reflected from the defect, that is

$$h_{opt} = \sum_{i=1}^{J} A_i s_0(t - t_i). \tag{4}$$

the SNR of the filter output $y(t)$ will be maximized. However, the defect echoes $s_d = \sum_{i=1}^{J} A_i s_0(t - t_i)$ are unknown, because the number of point reflectors *J*, the delays t_i and the amplitude factors A_i are all unknown. The goal of the optimal matched filter design is to tune the parameters of the filter response $h(t)$ to approximate the unknown defect echoes and obtain an optimal matched filter, so that the output SNR is maximized for a set of given training return signals.

In mathematics, the above problem of optimal matched filter design can be formulated by the following equations:

$$\max_{A_i, t_i} \mathrm{SNR}\left[y(t)\right] \quad \text{subject to} \quad \begin{aligned} y(t) &= h(t) * x(t) \\ h(t) &= \sum_{i=1}^{K} A_i s_0(t - t_i) \\ x(t) &= \sum_{i=1}^{J} A_i s_0(t - t_i) + n(t) \end{aligned} \tag{5}$$

where *K* is the number of point reflectors under consideration in the approximation to reconstruct the defect echo, which is unknown *a prior* and is a design parameter. In our previous work [5], the defect echoes was reconstructed using the excitation signals measured in the real scenario, which are accurate to account for the practical experimental uncertainties, but are also proven to be troublesome requiring extra efforts and time consuming. In this paper, we present a more robust and flexible design method which uses simulated excitation signals taking into account of the operation parameters of the transducer and the transmitter-receiver system, to approximate the defect echoes, and the experimental results obtained from the real industrial samples demonstrate that through the optimization and tuning procedure of the filter parameters, the same good results are obtained from this design routine.

From the problem formulation of optimal matched filter design (5), it demonstrates that the filter response determination consists of two steps: 1) To reconstruct the return echo by using the simulated excitation signal $s_0(t)$

and the design parameters K, A_i and t_i, $i=1, 2, \ldots, K$; and 2) Tweak the above control parameters until the output SNR is maximized.

We use an example to illustrate reconstruction of the return echoes using the simulated excitation signals in Step 1). Assume a typical commercial 5 MHz array with 64 elements to be considered. The array has an element pitch of 0.7 mm. The output from the excitation circuit is a short pulse, and the output of each element is a Gaussian windowed tone burst with a center frequency of 5 MHz and a -6 dB bandwidth of 70%. The transmitting and receiving elements are Element 6 and 50 respectively, and the velocity of sound is 5262 m/s. The sampling frequency is 100 MHz. There is a defect modelled by 5 point reflectors in a test sample of homogeneous and lossless material. The first element of the array is defined to be the origin of the coordinate system. The coordinates of the point reflectors, the simulation setup and the array parameters are detailed in Table 1 & 2 and Fig. 1.

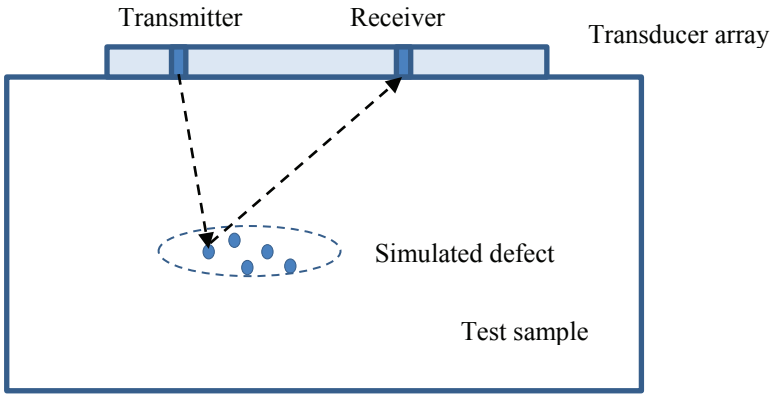

FIGURE 1. Simulation setup and illustration.

TABLE 1. Array parameters.

Array Parameters	Value
Number of Elements	64
Element Width	0.7 mm
Center Frequency	5 MHz
Bandwidth (-6 dB)	70%

TABLE 2. Coordinates and amplitude factors of point reflectors.

	Coordinate	Amplitude Factor
Point Reflector 1	(10, 100) mm	0.9
Point Reflector 2	(13, 95) mm	1.0
Point Reflector 3	(14.5, 105) mm	0.8
Point Reflector 4	(17, 100) mm	0.4
Point Reflector 5	(20, 105) mm	0.9

The illustrations of the simulated tone burst in the time domain and the frequency domain are shown in Fig. 2. The propagation distance from the transmitter to each reflector and back to the receiver is calculated using the coordinates, and then the propagation time is determined by dividing the propagation distance by the longitudinal velocity of the sound in the media. The return echo at the receiver is determined by the superposition of the 5 individual return signals from each point reflector with particular amplitude factor to address the element directivity and beam spread. The reconstructed return echo is demonstrated in Fig. 3, in the time domain and frequency domain, respectively.

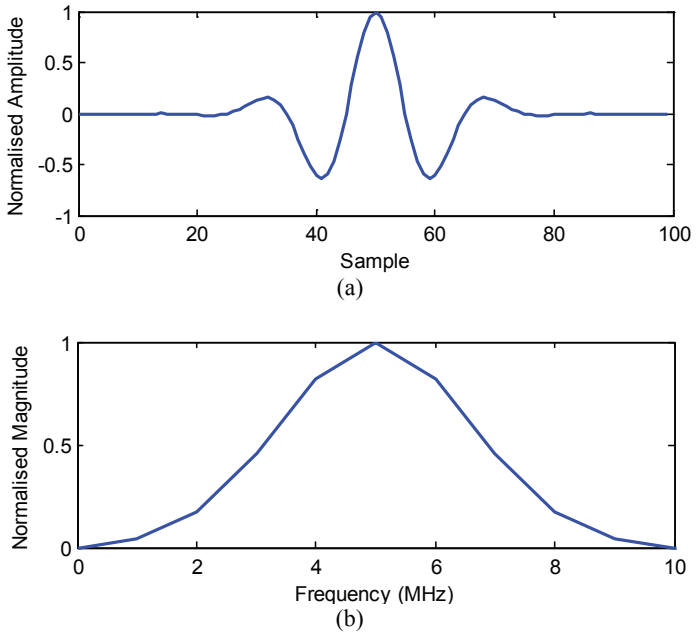

FIGURE 2. Simulated excitation signal. (a) In time domain, and (b) In frequency domain.

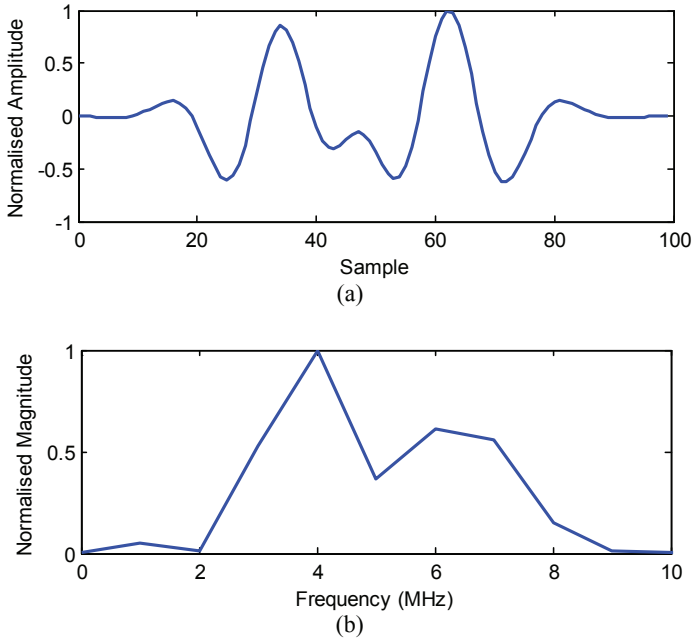

FIGURE 3. Simulated return echo. (a) In time domain, and (b) In frequency domain.

With a particular set of control parameters K, A_i and t_i, $i=1, 2, \ldots, K$, the return echo can be reconstructed, which can then be employed in the matched filter (5) and the output SNR can be calculated. The SNR will be increased or decreased depending on response of the filter. The second step of optimal matched filter design involves tweak the parameters by searching the best values in the problem space, in order to achieve the best SNR gain.

Apparently, the search process is not trivial, and the dependence of the cost function $\mathrm{SNR}\left[y(t)\right]$ in equation (5) on the control variables A_i and t_i is supposed to be non-linear, high-dimensional and complicated. As a result, a numerical optimization paradigm such as the Genetic Algorithms (GA), Simulated Annealing (SA), or Particle

Swarm Optimization (PSO) is in a good position to tackle this problem. Due to the space constraints, the numerical optimization algorithms are not discussed in details in this paper, but the readers may refer to [14, 15] and the references therein for more details about design of the routines and selection of the control parameters.

EXPERIMENTAL VERIFICATION

In this section, we analyze the performance of the optimal matched filter designed using the simulated broadband excitation signals for ultrasonic NDE imaging and defect detection, and compare with the design method based on the actual excitation signal in [5], as well as the gold-standard TFM technique [1]. The experimental setup employed in this work consists of 3 components, namely, the test sample, the ultrasound array transducer, and the phased array control system and a personal computer for excitation and signal processing. A 128-element transducer array with 0.7 mm element pitch and 5 MHz central frequency (Vermon, Tours, France) is utilized in contact with the test sample upper surface with gel coupling, as shown in Fig. 4(a). An OPEN ultrasonic phased array control system with 128 independent parallel channels and 16-bit resolution (LeCouer, Chuelles, France) is connected with the transducer array for excitation and data acquisition, as shown in Fig. 4(b). A personal computer is then connected to the OPEN system to control the excitation sequence and record the return signals for post processing and imaging. A MATLAB (The MathWorks, Natick, MA) routine is developed to implement the Full Matrix Capture (FMC) data acquisition, where each transducer element is excited sequentially and the echoes received by all the array elements are recorded [1]. A complete FMC data set is composed of N^2 A-scan waveforms, where N is the number of array elements.

In the experiments, the number of point reflectors K is pre-determined, which seems to be not highly sensitive to the performance, provided that a reasonably large K is employed, for example $K=15$. The matched filter response is approximated using equation (5) with K reflectors and all the unknown parameters are captured in a vector with a dimension of $2K$, i.e. A_i and t_i, $i=1, 2, ..., K$. The Particle Swarm Optimization (PSO) paradigm is employed in this work to tackle the problem at hand, because PSO is quite simple to implement, but it is as powerful as other popular evolutionary algorithms like the Genetic Algorithms, and is robust to the selection of control parameters [16]. The key parameters used in the PSO routine are summarized in Table 3, and the convergence is observed in all the experiments within the maximum number of iterations.

TABLE 3. PSO parameters.

PSO Parameters	Value
K	15
Number of Particles	150
Number of Iterations	500
c_1	0.4
c_2	1.2
Inertia Weight	0.8

(a) (b)

FIGURE 4. Experimental setup. (a) Transducer array and test sample, and (b) OPEN phased array control system.

A test sample with a thickness of around 150 mm made of INCONEL Alloy 617 is employed in this experiment. As illustrated in the datasheet, INCONEL Alloy 617 is a solid-solution, nickel-chromium-cobalt-molybdenum alloy with an exceptional combination of high-temperature strength and oxidation resistance, and it is readily formed and welded by conventional techniques [17]. Alloy 617 is widely used in a variety of key industrial sectors like Energy, Oil and Gas, and Nuclear for components such as ducting, combustion cans and transition liner. The FMC data set is recorded at a sampling rate of 100 MHz, and each A-scan waveform is band-pass filtered to remove the DC drift and high frequency noise. Due to the size of microstructure grain, Alloy 617 is demonstrated to be highly scattering to 5 MHz ultrasound, and results in dominant and significant grain noise and pretty low SNR.

Fig. 5(a) shows the A-scan waveform of the return signal at Element 20, the reflection from a major defect happens around the samples of 1650-1800. Due to the dominant grain noise, it is almost impossible to identify this reflection, and the SNR is measured to be -3 dB. Fig. 6(a) demonstrates the image obtained with the Total Focusing Method (TFM) [1] using the band-pass filtered FMC data set in a dynamic range of 40 dB. The image is pretty noisy and the back-wall is only partially visible at the depth of 147 mm.

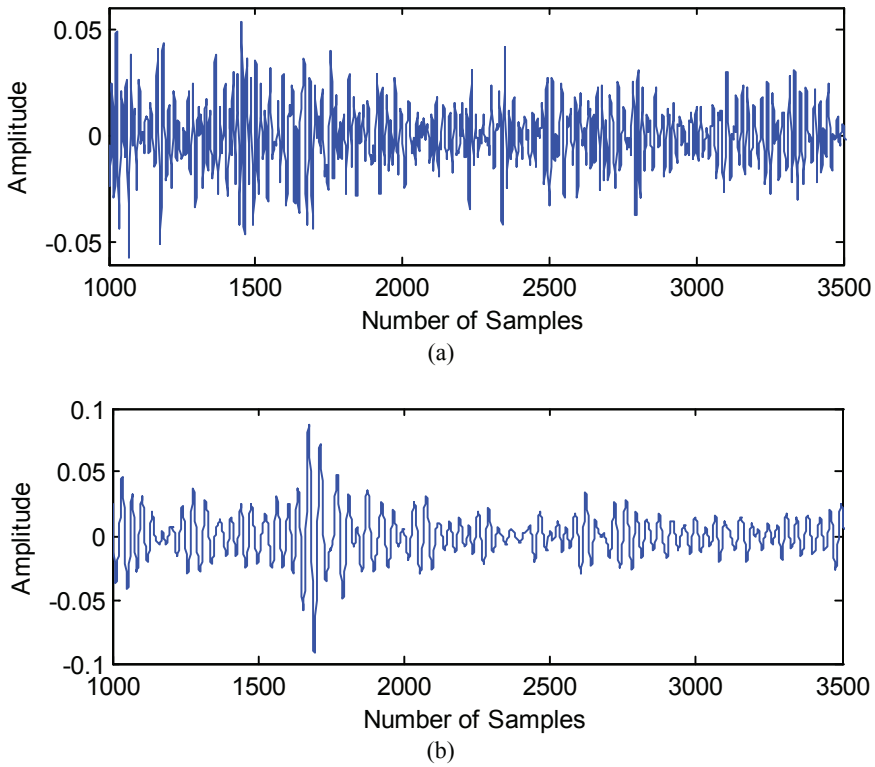

FIGURE 5. A-scan waveforms at Element 20. (a) Original, and (b) Matched filtered.

Fig. 5(b) illustrates the waveform at Element 20 processed with the optimized matched filter. Comparing to the original signal in Fig. 5(a), it is evident that the target echo has been enhanced and the grain noise has been suppressed with matched filtering, and it becomes much more confident to detect the defect from the amplitude. In terms of quantitative comparison, the SNR is increased to 3 dB, and the matched filter observes 6 dB SNR gain for the A-scan signals. To form the image in Fig. 6(b), firstly, each individual A-scan waveform in the FMC data set is matched filtered, and then the processed FMC data set is imaged with TFM. Comparing to the image in Fig. 6(a), it is evident that the clutter noise is greatly reduced, while the back wall reflection is further enhanced.

The matched filter works in the temporal-spectral domain. A variety of beamforming methods that exploit the spatial diversity and filtering, like the Capon beamformer [1], were investigated in the literature. There is a potential to combine these two categories of techniques since they work in different domains and may complement with each other for noise reduction. Fig. 6(c) shows the image obtained with the adaptive Capon beamformer using the matched filtered FMC data set. It is evident that the clutter noise is further reduced, and the back-wall reflection is

greatly enhanced in term of the strength as well as the visible lateral length, due to exploiting both the temporal and spatial information.

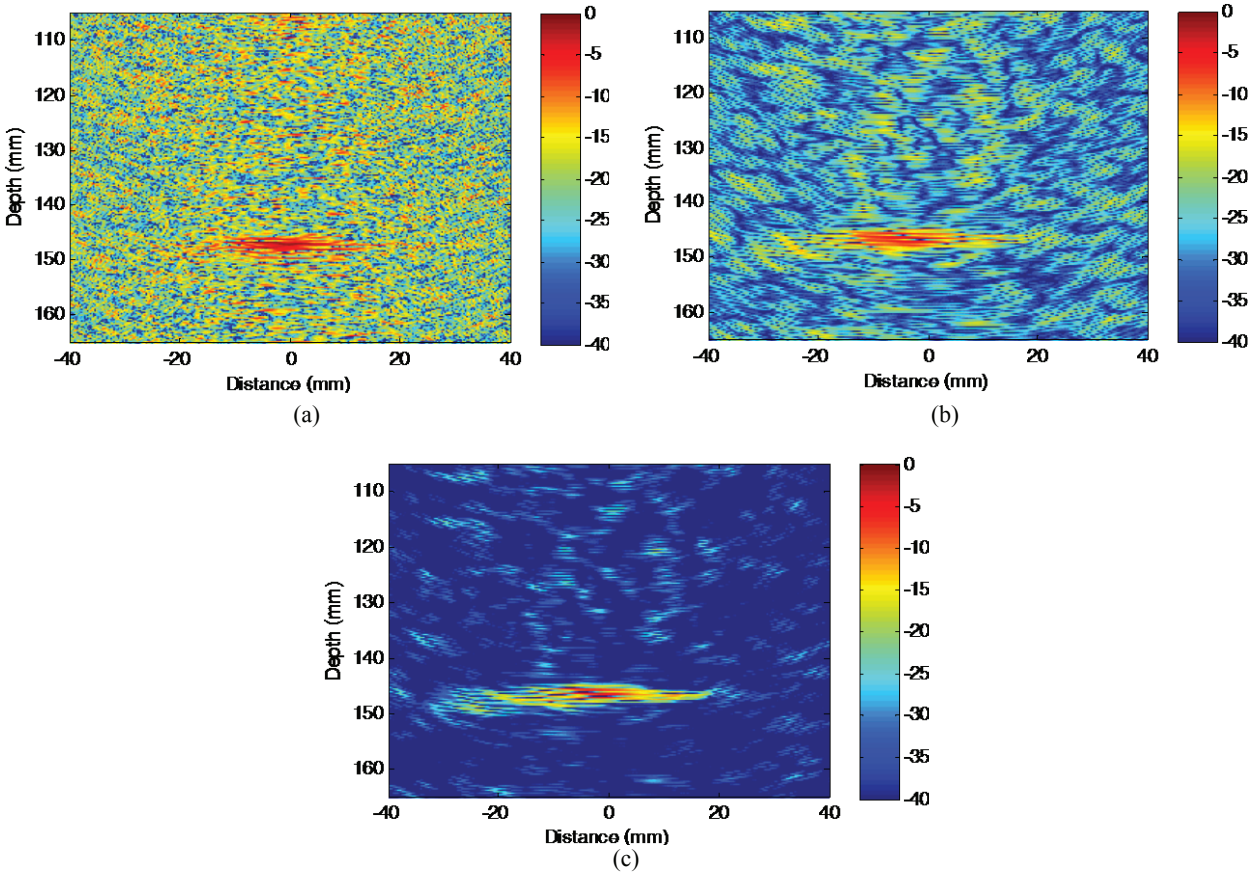

FIGURE 6. Images of Alloy 617 test block. (a) TFM with original FMC data set, (b) TFM with matched filtered FMC data set, and (c) Adaptive beamforming with matched filtered FMC data set.

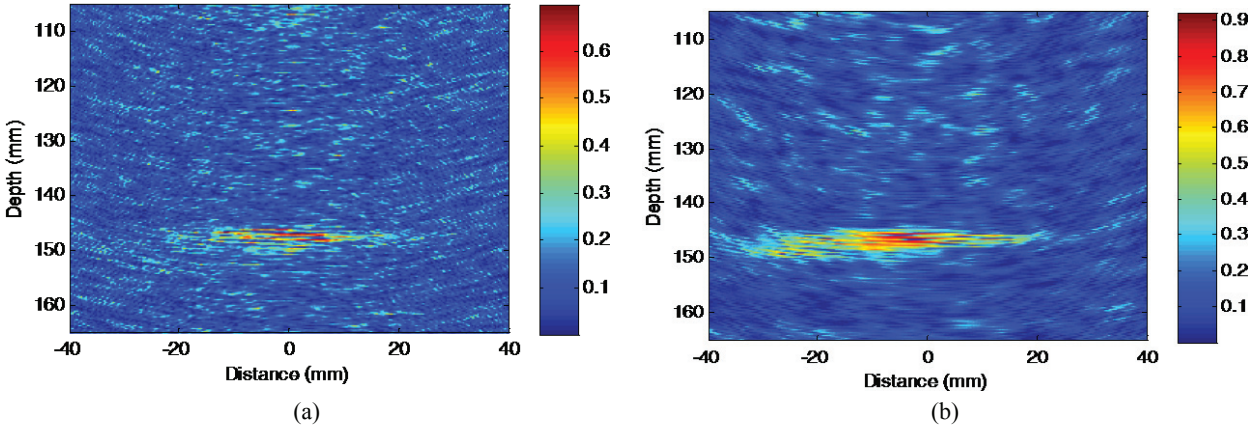

FIGURE 7. Coherence factors of Alloy 617 test block. (a) Computed with original data set, and (b) Computed with matched filtered data set.

The Coherence Factor (CF) computed with the FMC data set has been used as an important index to measure the quality of array focusing. The CF computes the factor of the energy of the coherent sum obtained in conventional delay-and-sum beamforming to the total incoherent energy that is N times the incoherent sum [18, 19]. Fig. 7(a) and Fig. 7(b) illustrate the CFs obtained with the original FMC data set and the matched filtered FMC data set, respectively. As can be seen from the figures, the CFs corresponding to the back wall are greatly improved which demonstrate a much longer lateral length, the maximum CF value is increased from 0.69 to 0.92, and the CFs corresponding to the grain noise are somewhat reduced. It is evident that the focusing quality by conventional delay-and-sum beamforming is greatly improved although the matched filter is applied to each A-scan waveform individually.

CONCLUSIONS AND FUTURE WORK

In the literature, matched filtering has been demonstrated to be a powerful yet efficient method to enhance defect detection and imaging in ultrasonic NDE of coarse grain materials, if the matched filter is properly designed and optimized to effectively approximate the defect echoes. The existing design method requires measuring the real excitation signals from the transducer element, which makes it time consuming and less straightforward to implement in practice. In this paper, we present a flexible and robust approach to optimal matched filter design using the simulated excitation signals, and the control parameters are optimized based on the real scenario of the array transducer, the transceiver system response, and the test sample, as a result, the optimal filter response depends on the material characteristics. Experiments on industrial samples of INCONEL Alloy 617 are conducted and the results confirm the advantages and robustness of the approach. The number of point reflectors K has been chosen as a design parameter and pre-determined in this work, the adaptive determination of an optimal K will be considered in the future improvement, and the enhanced version will be investigated on a variety of industrial samples of alloys, composites and stainless steel.

REFERENCES

1. M. Li and G. Hayward, "Ultrasound non-destructive evaluation (NDE) imaging with transducer arrays and adaptive processing," *Sensors* **12** (1) pp. 42-54, (2012).
2. M. Li, G. Hayward and B. He, "Adaptive array processing for ultrasonic non-destructive evaluation," *2011 IEEE International Ultrasonics Symposium (IUS) Proceedings*, (Orlando, FL, USA, October, 2011), pp. 2029-2032, (2011).
3. J. Camacho, M. Parrilla andC. Fritsch, "Phase coherence imaging," *IEEE Transactions on Ultrasonics, Ferroelectrics, and Frequency Control* **56** (5), pp. 958-974, (2009).
4. K. Ho, M. Li, R. O'Leary and A. Gachagan, "Application of frequency compounding to ultrasonic signals for the NDE of concrete," in *Review of Progress in Quantitative Nondestructive Evaluation*, eds. D. O. Thompson and D. E. Chimenti, (American Institute of Physics 1430, Melville, NY), **31**, pp. 1508-1515, (2012).
5. M. Li and G. Hayward, "Optimal matched filter design for ultrasonic NDE of coarse grain materials," in *Review of Progress in Quantitative Nondestructive Evaluation*, eds. D. E. Chimenti and L. J. Bond, (American Institute of Physics 1430, Melville, NY), **35**, pp. 020011 1-9, (2016).
6. M. Li and G. Hayward, "A rapid approach to speckle noise reduction in ultrasonic non-destructive evaluation using matched filters," *2014 IEEE International Ultrasonics Symposium (IUS) Proceedings*, (Chicago, IL, USA, September, 2014), pp. 45-48, (2014).
7. K. Srinivasan, C. P. Chiou, and R. B. Thompson, "Ultrasonic flaw detection using signal matching techniques," in *Review of Progress in Quantitative Nondestructive Evaluation*, eds. D. O. Thompson and D. E. Chimenti, (Plenum Press, NY), **14**, pp. 711-718 (1995).
8. N. Ruiz-Reyes, P. Vera-Candeas, J. Curpian-Alonso, R. Mata-Campos, and J. C. Cuevas-Martinez, "New matching pursuit-based algorithm for SNR improvement in ultrasonic NDT," *NDT&E International* **38**(6) pp. 453-458 (2005).
9. M. Li and Y. Lu, "Improving the performance of GA-ML DOA estimator with a resampling scheme," *Signal Processing* **84** (10) pp. 1813-1822, (2004).

10. M. Li and Y. Lu, "Source bearing and steering-vector estimation using partially calibrated arrays," *IEEE Transactions on Aerospace and Electronic Systems* **45** (4), pp. 1361-1372, (2009).
11. M. Li and Y. Lu, "Optimal direction finding in unknown noise environments using antenna arrays in wireless sensor networks," *7th International Conference on Intelligent Transportation Systems Telecommunications (ITST2007) Proceedings*, (Sophia Antipolis, France, June, 2007), pp. 332-337, (2007).
12. M. Li, K. S. Ho and G. Hayward, "Accurate angle-of-arrival measurement using particle swarm optimisation," *Wireless Sensor Network* **2**(5) pp. 358-364, (2010).
13. C. Holmes, B. Drinkwater and P. Wilcox, "Post-processing of the full matrix of ultrasonic transmit-receive array data for non-destructive evaluation," *NDT&E International* **38**(8), pp. 701-711, (2005).
14. M. Li and Y. Lu, "Maximum likelihood DOA estimation in unknown colored noise fields," *IEEE Transactions on Aerospace and Electronic Systems* **44** (3), pp. 1079-1090, (2008).
15. M. Li and Y. Lu, "A refined genetic algorithm for accurate and reliable DOA estimation with a sensor array," *Wireless Personal Communications* **43** (2) pp. 533-547, (2007).
16. R. Eberhart and J. Kennedy, "A new optimizer using particle swarm theory," *6th International Symposium on Micro Machine and Human Science Proceedings*, (Nagoya, Japan, October, 1995), pp.39-43, (1995).
17. INCONEL 617 Technical Data, http://www.hightempmetals.com/techdata/hitempInconel617data.php, accessed in September 2016.
18. P.-C. Li and M.-L. Li, "Adaptive imaging using the generalized coherence factor," *IEEE Transactions on Ultrasonics, Ferroelectrics, and Frequency Control* **50** (2), pp. 128-141, (2003).
19. T. Lardner, M. Li and A. Gachagan, "Using phase information to enhance speckle noise reduction in the ultrasonic NDE of coarse grain materials," in *Review of Progress in Quantitative Nondestructive Evaluation*, eds. D. E. Chimenti, L, J. Bond and D. O. Thompson, (American Institute of Physics 1581, Melville, NY), **33**, pp. 1061-1069, (2014).